Electronic Supplementary Material (ESI) for ChemComm.

Electronic Supporting Information

Crystalline Fibres of a Covalent Organic Framework through bottom-up Microfluidic Synthesis

David Rodríguez-San-Miguel,[†a] Afshin Abrishamkar,[†b,c] Jorge A. R. Navarro,[d] Romen Rodriguez-Trujillo,[e] David B. Amabilino,[f] Ruben Mas-Ballesté,*[a] Félix Zamora*[a,g,h] and Josep Puigmartí-Luis,*[b]

[a] *Departamento de Química Inorgánica. Universidad Autónoma de Madrid. 28049 Madrid, Spain. E-mail: ruben.mas@uam.es; felix.zamora@uam.es.*

[b] *Empa, Swiss Federal Laboratories for Materials Science and Technology, Lerchenfeldstrasse 5, 9014 St. Gallen, Switzerland. E-mail: josep.puigmarti@empa.ch*

[c] *Department of Chemistry and Applied Biosciences, Institute for Chemical and Bioengineering, ETH Zurich, Vladimir Prelog Weg 1, 8093 Zurich, Switzerland.*

[d] *Departamento de Química Inorgánica, Universidad de Granada, 18071 Granada, Spain.*

[e] *Institut de Ciència de Materials de Barcelona (ICMAB-CSIC), Campus Universitari de Bellaterra, 08193 Cerdanyola del Vallès, Catalonia, Spain.*

[f] *School of Chemistry, The University of Nottingham, University Park, NG7 2RD, United Kingdom.*

[g] *Condensed Matter Physics Center (IFMAC), Universidad Autónoma de Madrid. 28049 Madrid, Spain.*

[h] *Instituto Madrileño de Estudios Avanzados en Nanociencia (IMDEA Nanociencia), Cantoblanco, 28049 Madrid, Spain.*

[†] *These authors contributed equally to this work.*

Table of Contents

Section A. Materials and Methods

The PDMS base and curing agent were purchased from Dow Corning (Sylgard 184 Silicone elastomer kit). 1,3,5-benzenetricarboxaldehyde was obtained from Manchester Organics. 1,3,5-tris-(4'-aminophenyl)benzene was prepared according to literature procedures.[1] HPLC grade methanol was purchased from Fisher Chemical. Other chemicals and solvents were obtained from Sigma-Aldrich and used without further purification unless specified.

Microfluidic device fabrication: The silicon master mold used for the fabrication of the microfluidic chips was produced using standard photolithography techniques as described in detail elsewhere.[2] The microfluidic chips employed in this work were fabricated through a conventional polydimethylsiloxane (PDMS) replica molding process. In brief, a mixture of PDMS base and curing agent 10:0.9 ratio by weight was casted against the silicon master mold, previously passivated with chlorotrimethylsilane under vacuum for 30 min, and was then cured at 70 ºC for 3 hours. Next, the cured PDMS was peeled off from the master mold and cut with a razor blade resulting in a PDMS slab with channel features and dimensions of 24 × 24 mm^2. The four inlets and the outlet channel of the PDMS slab were punched with a biopsy punch (1.5 mm, Miltex GmBH, Germany) and subsequently bonded against a glass coverslip (24 × 40 mm^2, #5, Menzel-Glaser, Germany) using a laboratory corona discharge (BD-20ACV, Electro-Technic Products, USA). Finally, the bonding was further facilitated by heating the assembled structure at 70 ºC for 4 hours.
The microfluidic device used in this work was comprised of four converging input channels and one main reactor channel. The height of all channels was 50 µm and the main channel length was set at 1 cm. The width of the four input channels and main channel were 50 µm and 250 µm, respectively.

ATR-FT-IR Spectroscopy: ATR-FT-IR spectroscopy was recorded in a Perkin Elmer Spectrum 100 with a PIKE Technologies MIRacle Single Reflection Horizontal ATR Accesory with a spectral range of 4000-650 cm^{-1}.

Solid-State ^{13}C CP-MAS Nuclear Magnetic Resonance Spectroscopy. High resolution solid-state nuclear magnetic resonance (NMR) spectra were recorded at ambient pressure on a Bruker AV 400 WB spectrometer using a triple channel (BL4 X/Y/^{1}H) and Bruker magic angle-spinning (MAS) probe with 4 mm (outside diameter) zirconia rotors. The magic angle was adjusted by maximizing the number and amplitudes of the signals of the rotational echoes observed in the ^{79}Br MAS FID signal from KBr. Cross-polarization with MAS (CP-MAS) was used to acquire ^{13}C data at 100.61 MHz. The ^{1}H ninety degree pulse widths were both 3.1 µs. The CP contact time varied from 3.5 ms. High power two-pulse phase modulation (TPPM) 1H decoupling was applied during data acquisition. The decoupling frequency corresponded to 80 kHz. The MAS sample spinning rate was 10 kHz. Recycle delays between scans were 4 s. The ^{13}C chemical shifts are given relative to tetramethylsilane as zero ppm, calibrated using the methylene carbon signal of adamantane assigned to 29.5 ppm as secondary reference.

Thermogravimetry. Thermogravimetric analyses of samples were run on a Thermobalance TGA Q-500 thermal gravimetric analyzer with samples held in a platinum pan under nitrogen atmosphere. A 10 K min-1 ramp rate was used.

Elemental Analysis: Elemental analyses were obtained using LECO CHNS-932 elemental analyzer.

Powder X-Ray Diffraction: PXRD patterns were collected with a Bruker D8 Advance X-ray diffractometer (Cu-Kα radiation; λ = 1.5418 Å) equipped with a Lynxeye detector. Samples were mounted on a flat sample plate. Patterns were collected in the $3.5° < 2\theta < 35°$ range with a step size of 0.016° and exposure time of 0.8 s/step.

Field-Emission Scanning Electron Microscopy: FESEM studies were performed on a Philips XL 30 S-FEG microscope operating at an accelerating voltage of 10 kV. Samples were previously coated with chromium in a sputter Quorum Q150T-S.

Transmission Electron Microscopy: TEM studies were performed on a JEOL JEM-2100 microscope operating at 200 kV. Samples were prepared by sonicating in methanol at 35 kHz for 10 minutes a small piece of MF-COF-1 as obtained directly from the outlet of the microfluidic device. Then, a drop of the suspension was poured over a TEM grid (200 mesh, gold-based holey carbon film, Quantifoil®)

Gas Adsorption: Conventional adsorption isotherms were measured using a Micromeritics Tristar 3000 volumetric instrument under continuous adsorption conditions. Brunauer-Emmet-Teller (BET) and Langmuir analyses were carried out to determine the total specific surface areas for the N_2 isotherms at 77 K. Prior to measurement, powdered samples were heated at 423 K for 12 h and outgassed to 10^{-6} Torr.

Section B. Synthetic Procedures

RT-COF-1. 100 mg (0.285 mmol) of 1,3,5-tris(4'-aminophenyl)benzene (TAPB) were dissolved in 6 mL of *m*-cresol. 46.1 mg (0.285 mmol) of 1,3,5-benzenetricarboxaldehyde (BTCA) were dissolved in 4 mL of *m*-cresol and 1 mL of glacial acetic acid. Both solutions were subsequently mixed at room temperature. It was observed, almost immediately, the formation of a yellow gel. After 30 minutes, the gel was washed with tetrahydrofuran (4x100 mL) and methanol (4x100 mL) and isolated by filtration. The resulting solid was dried under open atmosphere over 2 days. The solid obtained was dried under vacuum (50 mbar) at 150 ºC for 24 h to yield 126 mg (96 % yield) of RT-COF-1 as a yellow solid. Elemental analysis calculated for $C_{33}H_{21}N_3 \cdot 2.5H_2O$: C: 78.47 %, H: 5.29 %, N: 8.32 %. Found: C: 78.59 %, H: 4.91 %, N: 8.57 %.

RT-COF-1Ac. 100 mg (0.285 mmol) of TAPB were dissolved in 14.2 mL of glacial acetic acid. 46 mg (0.285 mmol) of BTCA were dissolved in 14.2 mL of glacial acetic acid. Both solutions were mixed at room temperature and an orange gel formed immediately. After 30 minutes, the gel was washed with tetrahydrofuran (4x100 mL) and methanol (4x100 mL) and isolated by filtration. The resulting solid was dried under open atmosphere over 2 days. The solid obtained was dried under vacuum (50 mbar) at 150 ºC for 24 h to yield 116 mg (89 % yield) of RT-COF-1 as a yellow solid. Elemental analysis calculated for $C_{33}H_{21}N_3 \cdot 0.5H_2O$: C: 84.43 %, H: 4.69 %, N: 8.96 %. Found: C: 83.07 %, H: 4.81 %, N: 8.72 %.[*]

MF-COF-1. Solutions in acetic acid of 1,3,5-benzenetricarboxaldehyde (0.040 M) and 1,3,5-tris-(4'-aminophenyl)benzene (0.040 M) were prepared and filtered using syringe filters with a pore size of 0.45 μm (Titan Syringe Filter, Fisher Scientific).
In a typical experiment, the solutions of 141 mg of TAPB in 10 mL acetic acid and 65 mg of BTCA in 10 mL acetic acid were injected into the two middle input channels of the microfluidic device (B and C in Fig. 1a in the main text) at a flow rate of 100 μL/min. In order to control the reaction time in the main channel, we supplied two sheath flows (Fig. 1a of the main text) of pure acetic acid that allow us to tune the flow focusing conditions, and thereby, the reaction time of the reagents along the main channel. For the synthesis of MF-COF-1 fibers, the flow rates of the sheath flows were optimized and maintained at 100 μL/min. All solutions were injected into the microfluidic device using a syringe pump system (neMESYS module, Cetoni GmbH Korbußen) that facilitated an accurate control of all the input flow rates, individually. Following the synthesis, the yellowish MF-COF-1 fibers were collected from the outlet

[*] **RT-COF-1Ac elemental analysis**: $0.5 \times H_2O$ is 1.9 % weight of water (volatiles) in the sample, which agrees with TGA.

of the microfluidic device and immersed in a petri dish filled with acetic acid. The fibers were washed with tetrahydrofuran (4×100 mL) and methanol (4×100 mL) and isolated by filtration. The resulting solid was dried under open atmosphere over 2 days. The solid obtained was dried under vacuum (50 mbar) at 150 ºC for 24 h to yield MF-COF-1 as an orange solid with 92 % yield. Elemental analysis calculated for $C_{33}H_{21}N_3 \cdot 0.75H_2O \cdot 1CH_3COOH$: C: 78.87 %, H: 4.98 %, N: 7.89 %. Found: C: 77.44 %, H: 4.90 %, N: 8.08 %.[*]

[*] **MF-COF-1 elemental analysis:** $0.75 \times H_2O$ is 2.54 % weight of water (volatiles) in the sample. Agrees with TGA assuming that acetic acid is strongly bound and does not release before COF decomposition start (*ca*. 350-400 ºC).

Section C. ATR-FT-IR Spectra

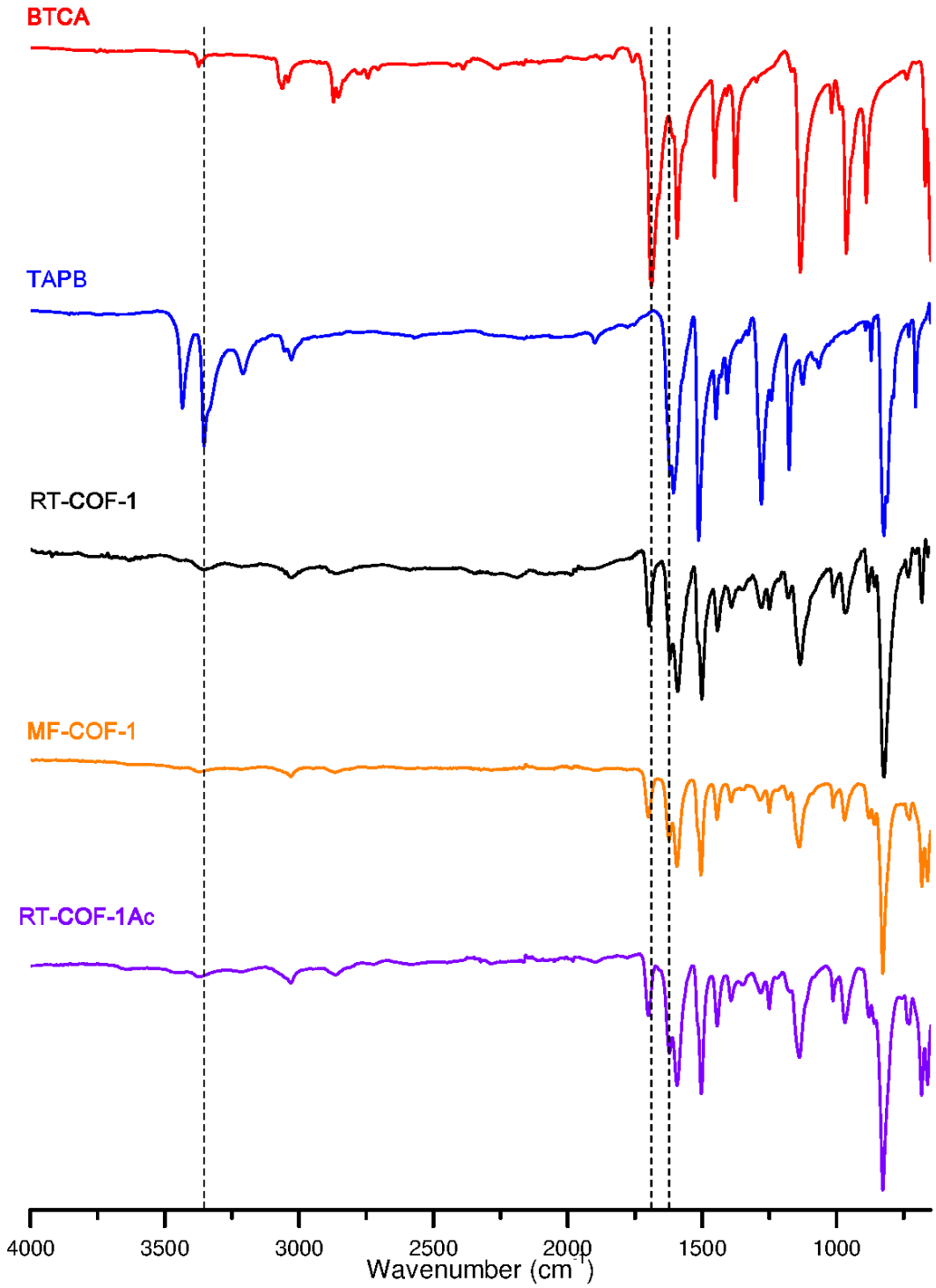

Fig. S1. ATR-FT-IR spectra of monomers **BTCA** (red) and **TAPB** (blue), of **RT-COF-1** (black), of MF-COF-1 (orange) and of **RT-COF-1Ac** (purple). The most significant changes are highlighted: Disappearance of N-H stretching bands between 3300-3500 cm^{-1}, decrease of the intensity of C=O stretching band at 1689 cm^{-1}, and appearance of C=N stretching band at 1623 cm^{-1}.

Section D. Solid State ^{13}C CP-MAS NMR Spectra

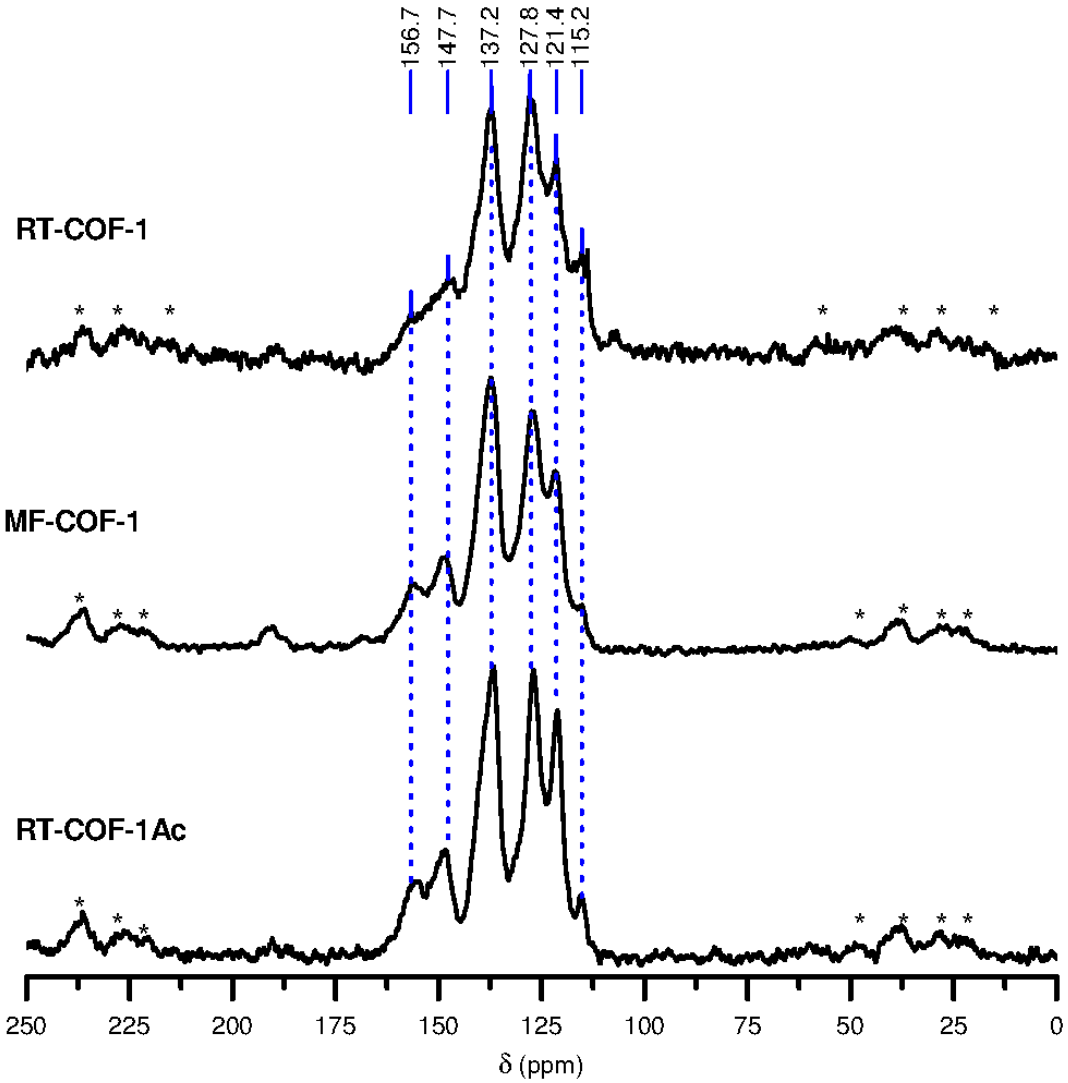

Fig. S2. Solid state ^{13}C CP-MAS NMR spectra of **RT-COF-1** (top), **MF-COF-1** (middle) and **RT-COF-1Ac** (bottom). Asterisks denote spinning sidebands.

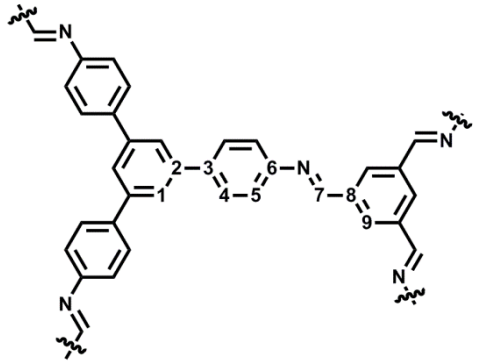

Signal (ppm)	Assignment
156.7	7
147.7	6
137.2	2, 3, 8
127.8	4, 9
121.4	1
115.2	5

Section E. Thermogravimetric analyses

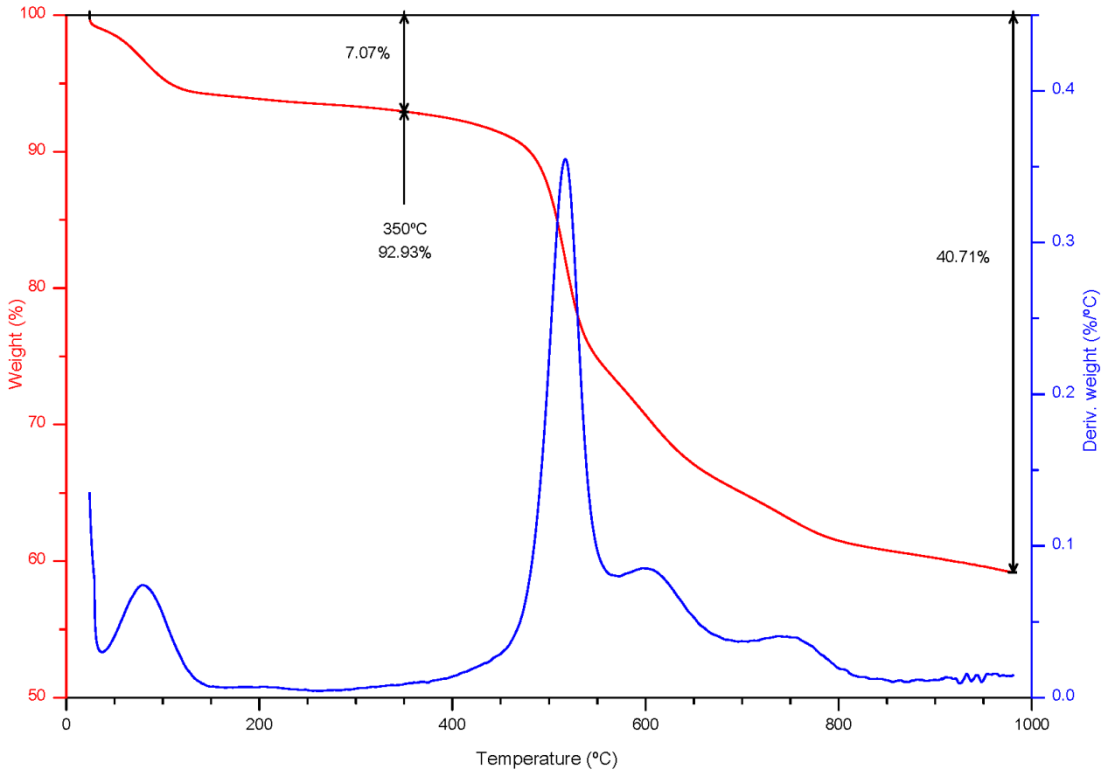

Fig. S3. TGA trace for **RT-COF-1**.

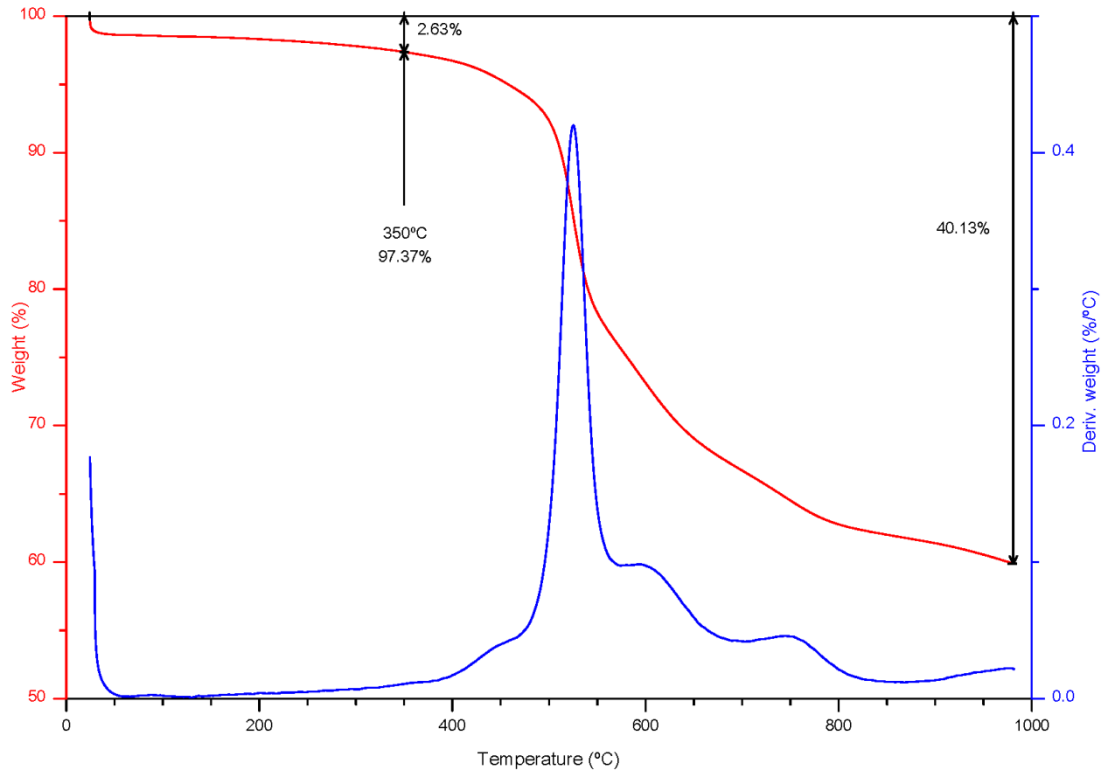

Fig. S4. TGA trace for **MF-COF-1**.

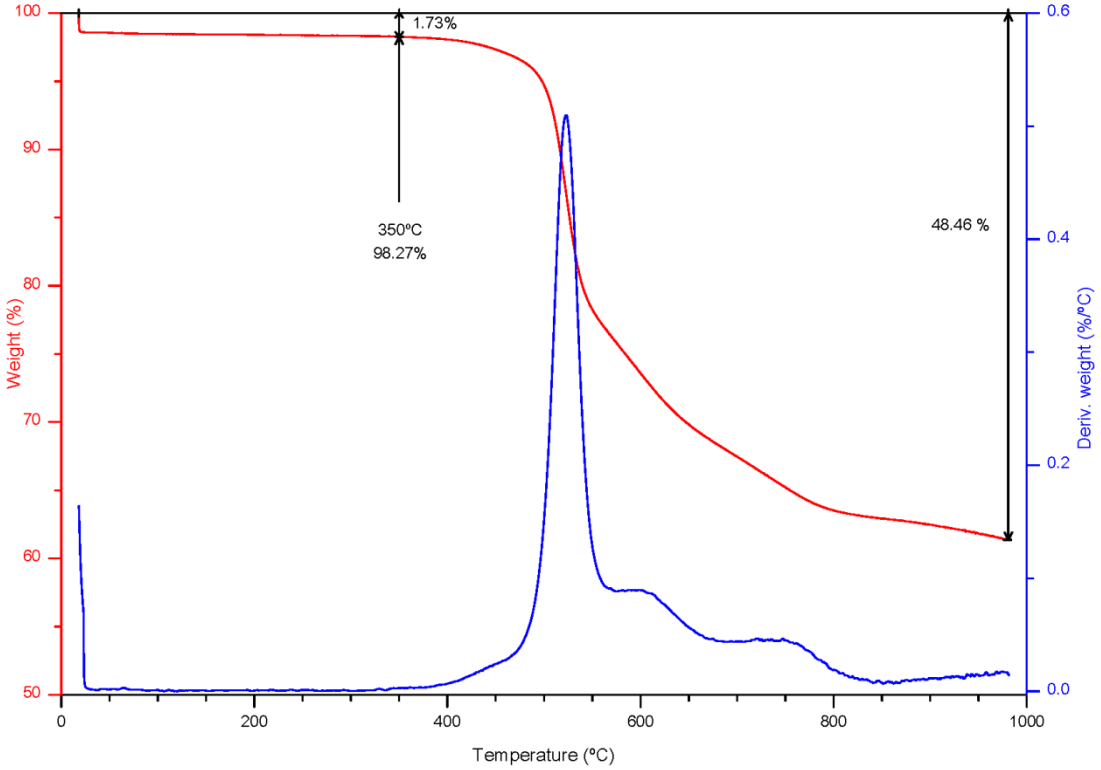

Fig. S5. TGA trace for **RT-COF-1Ac**.

Section F. Powder X-Ray Diffraction

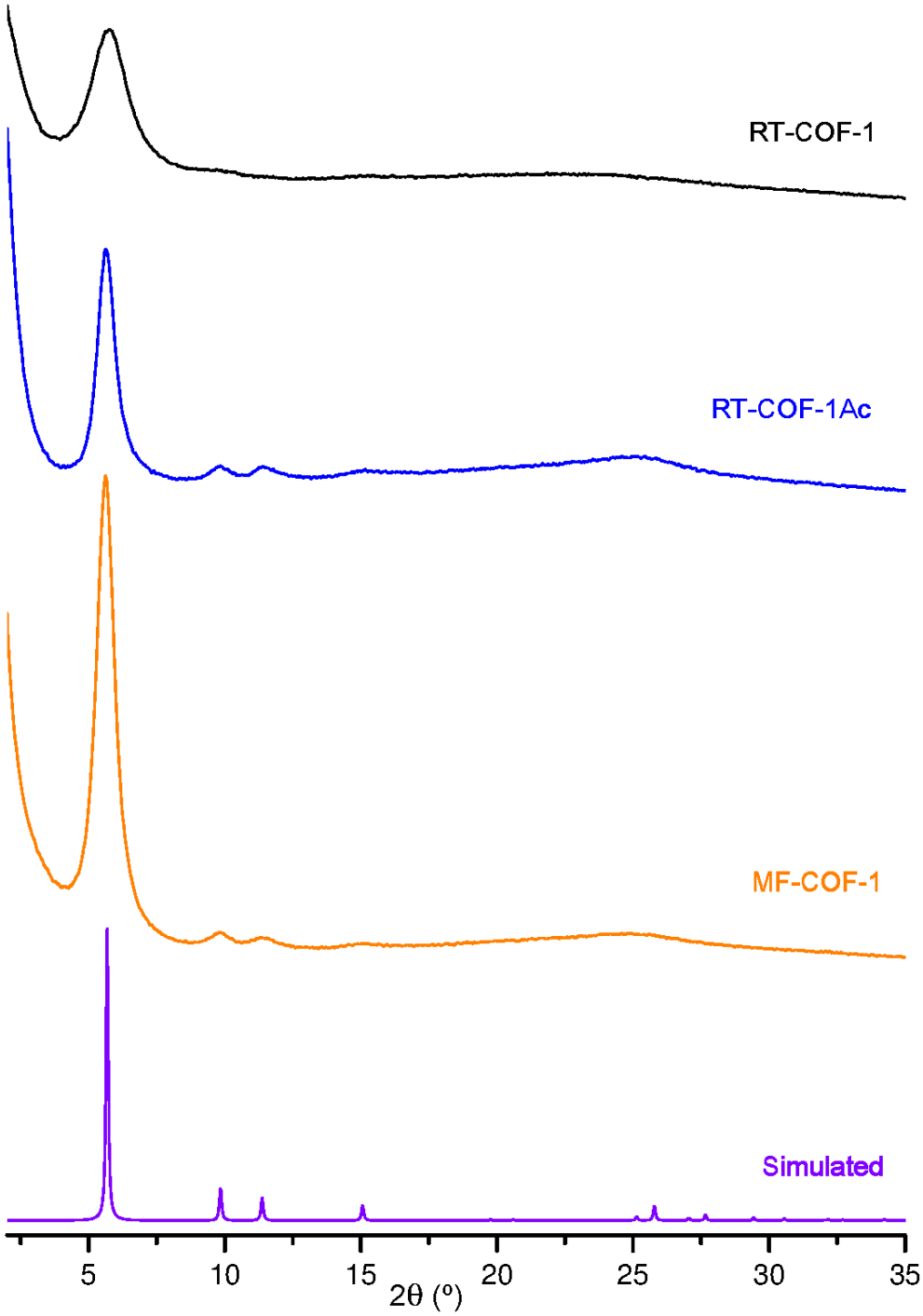

Fig. S6. PXRD patterns of **RT-COF-1** (black), **RT-COF-1Ac** (blue) and **MF-COF-1** (orange) and simulated PXRD pattern (purple).

Section G. Field Emission Scanning Electron Microscopy

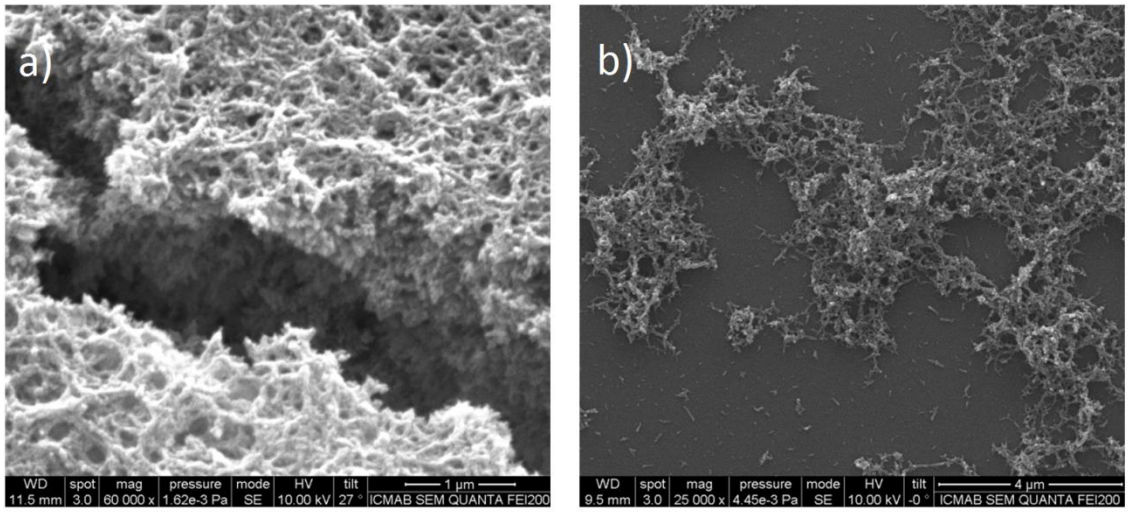

Fig. S7. FESEM images of **MF-COF-1** produced at FRR of 1 (a) and at FRR of 4 (b).

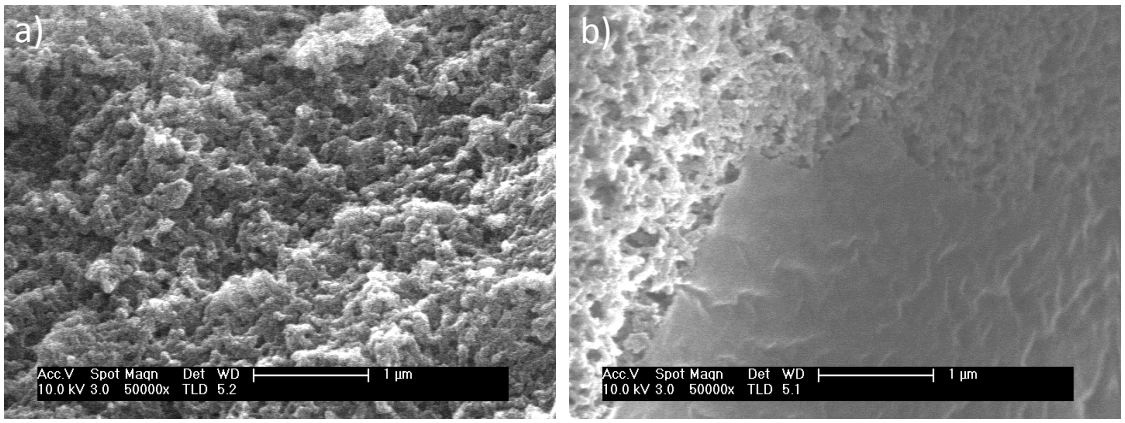

Fig. S8. FESEM images of **RT-COF-1Ac** showing (a) aggregated particles forming layer-like structures, and (b) a region where some particles have complete fused to form a sheet like structure.

Section H. N_2 adsorption.

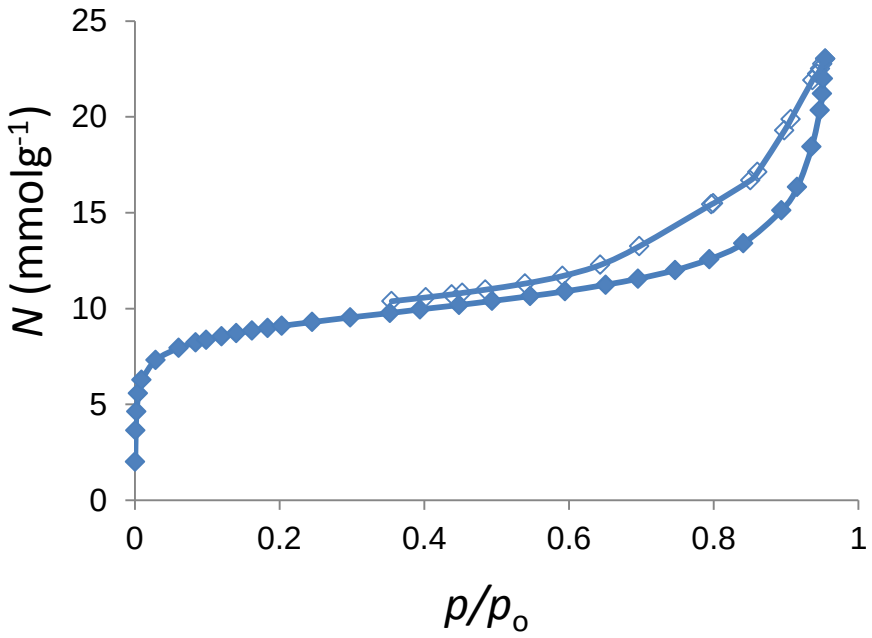

Fig. S9. N_2 isotherm for **RT-COF-1Ac** at 77 K; filled dots: adsorption, empty dots: desorption. The fitting of the data to BET equation gives rise to a specific surface area (SA) of 705 m^2g^{-1} while the fitting to Langmuir equation gives rise to an specific SA of 920 m^2g^{-1}.

Section I. Microfluidic set-up and a freestanding fiber.

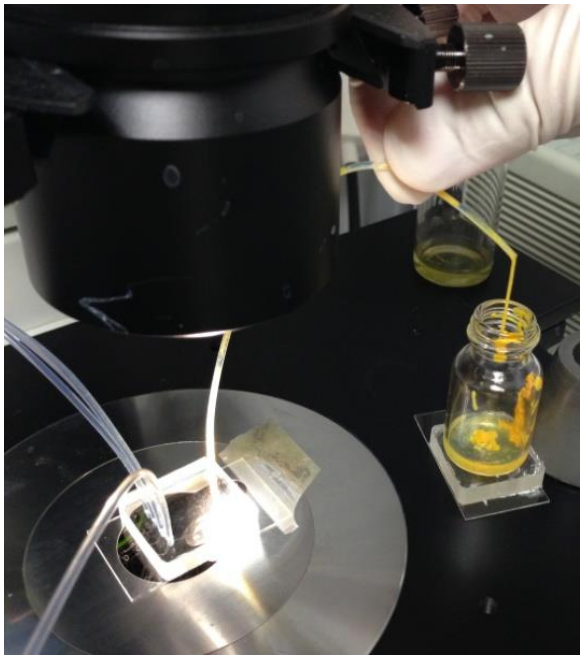

Fig. S10. Micrograph of the microfluidic reactor working in a continuous flow with a freestanding **MF-COF-1** fiber.

References

1. A. D. Ruigomez, D. Rodriguez-San-Miguel, K. C. Stylianou, M. Cavallini, D. Gentili, F. Liscio, S. Milita, O. M. Roscioni, M. L. Ruiz-Gonzalez, C. Carbonell, D. Maspoch, R. Mas-Balleste, J. L. Segura and F. Zamora, *Chem. Eur. J.*, 2015, **21**, 10666-10670.

2. A. Abrishamkar, M. Paradinas, E. Bailo, R. Rodriguez-Trujillo, R. Pfattner, R. M. Rossi, C. Ocal, A. J. deMello, D. B. Amabilino, J. Puigmartí-Luis, Microfluidic Pneumatic Cages: A Novel Approach for In-chip Crystal Trapping, Manipulation and Controlled Chemical Treatment., *J. Vis. Exp.*, 2016, e54193, doi:10.3791/54193